Molecular Dynamics Simulation of the Cross-Scale Role of the Transition Layer in Droplet Coalescence under a DC Electric Field

Chunhui Song, Huiru He, Wenjie Guo, Xu Cao, Junjia Zhu, Minghe Chi*

Chunhui Song, Huiru He, Wenjie Guo, Xu Cao, Junjia Zhu, Minghe Chi*

Key Laboratory of Engineering Dielectrics and Its Application, Ministry of Education, Harbin University of Science and Technology, Heilongjiang, China, 150080, P. R. China

*Corresponding author. E-mail: chiminghe1985@hrbust.edu.cn

S1. DC electric field application method

The electric field utilized in this study was generated by the built-in program within GROMACS software. The mathematical expression for this specific electric field is depicted in Eq. (S1).[1]

$$E(t) = E_0 \exp\left[-\frac{(t-t_{a0})^2}{2\sigma_p^{\,2}}\right]\cos\left[\omega_p (t-t_{a0})\right] \quad \text{(S1)}$$

where E_0 is the amplitude of electric field strength, t_{a0} is the time at the peak in the field strength, t is electric field application time, σ_p is the width of the pulse, and ω_p is the angular frequency. When σ_p=0 and ω_p=0, a DC electric field with a field strength of E_0 will be generated. The simulation system employed DC electric fields exclusively along the z-axis of the box.

S2. Force field parameters

The force field parameters for Span-80, n-hexane, water molecules and ions were shown in Table S1.[2,3]

The force-field parameters of Span80 listed in Table S1 were adopted from an established general force-field framework and relevant literature, and were assigned according to the molecular topology used in this work.[4] No separate reparameterization was performed for Span80 in this study, and the applicability of these parameters was mainly assessed based on the structural stability of the molecules and the reasonableness of their interfacial adsorption behavior during the simulations.

Table S1 Nonbonded interaction parameters.

$C_{24}H_{44}O_6$

Atom	C_6 (kJ mol^{-1} nm^6)	C_{12} (kJ mol^{-1} nm^{12})	Charge (e)
H44	8.464e-05	1.5129e-08	0.0481
C24	0.0023406244	4.937284e-06	-0.2379
H42	8.464e-05	1.5129e-08	0.0481
H43	8.464e-05	1.5129e-08	0.0481
C22	0.0023406244	4.937284e-06	0.2314
H38	8.464e-05	1.5129e-08	-0.0473
H39	8.464e-05	1.5129e-08	-0.0472
C19	0.0023406244	4.937284e-06	-0.0623
H34	8.464e-05	1.5129e-08	0.0015
H35	8.464e-05	1.5129e-08	0.0015
C16	0.0023406244	4.937284e-06	0.111
H28	8.464e-05	1.5129e-08	-0.0227
H29	8.464e-05	1.5129e-08	-0.0227
C13	0.0023406244	4.937284e-06	-0.1758
H24	8.464e-05	1.5129e-08	0.0491
H25	8.464e-05	1.5129e-08	0.0491
C14	0.0023406244	4.937284e-06	0.0445
H26	8.464e-05	1.5129e-08	0.0031
H27	8.464e-05	1.5129e-08	0.0031
C17	0.0023406244	4.937284e-06	-0.1579

H30	8.464e-05	1.5129e-08	0.0332
H31	8.464e-05	1.5129e-08	0.0332
C20	0.0023406244	4.937284e-06	0.2933
H36	8.464e-05	1.5129e-08	-0.0251
H37	8.464e-05	1.5129e-08	-0.0251
C23	0.0023406244	4.937284e-06	-0.3374
H41	8.464e-05	1.5129e-08	0.1479
C21	0.0023406244	4.937284e-06	-0.251
H40	8.464e-05	1.5129e-08	0.1186
C18	0.0023406244	4.937284e-06	0.1888
H32	8.464e-05	1.5129e-08	0.0059
H33	8.464e-05	1.5129e-08	0.0059
C12	0.0023406244	4.937284e-06	-0.2044
H22	8.464e-05	1.5129e-08	0.0481
H23	8.464e-05	1.5129e-08	0.0481
C10	0.0023406244	4.937284e-06	0.0641
H18	8.464e-05	1.5129e-08	0.0069
H19	8.464e-05	1.5129e-08	0.0069
C8	0.0023406244	4.937284e-06	-0.023
H14	8.464e-05	1.5129e-08	0.0086
H15	8.464e-05	1.5129e-08	0.0086
C7	0.0023406244	4.937284e-06	0.0091

H12	8.464e-05	1.5129e-08	0.0065
H13	8.464e-05	1.5129e-08	0.0065
C9	0.0023406244	4.937284e-06	0.0217
H16	8.464e-05	1.5129e-08	0.0324
H17	8.464e-05	1.5129e-08	0.0324
C11	0.0023406244	4.937284e-06	-0.4016
H20	8.464e-05	1.5129e-08	0.1367
H21	8.464e-05	1.5129e-08	0.1367
C15	0.002025	1e-06	0.7662
O6	0.00308914	4.77422e-06	-0.6026
O5	0.0022619536	1.21e-06	-0.4477
C6	0.002025	1e-06	0.1274
H7	8.464e-05	1.5129e-08	0.0711
H8	8.464e-05	1.5129e-08	0.0711
C4	0.0023406244	4.937284e-06	0.1106
H4	8.464e-05	1.5129e-08	0.1263
O4	0.00177494	1.21e-06	-0.6876
H11	0	0	0.4591
C1	0.0023406244	4.937284e-06	0.2188
H1	8.464e-05	1.5129e-08	0.0185
O1	0.0022619536	1.21e-06	-0.4594
C5	0.0023406244	4.937284e-06	0.0073

H5	8.464e-05	1.5129e-08	0.0802
H6	8.464e-05	1.5129e-08	0.0802
C3	0.0023406244	4.937284e-06	0.3395
H3	8.464e-05	1.5129e-08	-0.009
O3	0.00177494	1.21e-06	-0.7365
H10	0	0	0.445
C2	0.0023406244	4.937284e-06	0.283
H2	8.464e-05	1.5129e-08	0.0387
O2	0.00177494	1.21e-06	-0.7035
H9	0	0	0.406

C_6H_{14}

Atom	C_6 (kJ mol^{-1} nm^6)	C_{12} (kJ mol^{-1} nm^{12})	Charge (e)
H14	8.464e-05	1.5129e-08	0.069
C6	0.0023406244	4.937284e-06	-0.308
H12	8.464e-05	1.5129e-08	0.069
H13	8.464e-05	1.5129e-08	0.069
C5	0.002340624	4.94E-06	0.219
H10	8.464e-05	1.5129e-08	-0.037
H11	8.464e-05	1.5129e-08	-0.037
C4	0.002340624	4.94E-06	-0.058
H8	8.464e-05	1.5129e-08	0.007

H9	8.464e-05	1.5129e-08	0.007
C3	0.002340624	4.94E-06	-0.058
H6	8.464e-05	1.5129e-08	0.007
H7	8.464e-05	1.5129e-08	0.007
C2	0.002340624	4.94E-06	0.219
H4	8.464e-05	1.5129e-08	-0.037
H5	8.464e-05	1.5129e-08	-0.037
C1	0.002340624	4.94E-06	-0.308
H1	8.464e-05	1.5129e-08	0.069
H2	8.464e-05	1.5129e-08	0.069
H3	8.464e-05	1.5129e-08	0.069

H_2O

Atom	C_6 (kJ mol^{-1} nm^6)	C_{12} (kJ mol^{-1} nm^{12})	Charge (e)
OW	0.0026173456	2.634129e-06	-0.8476
HW1	0	0	0.4238
HW2	0	0	0.4238

Ions

Atom	C_6 (kJ mol^{-1} nm^6)	C_{12} (kJ mol^{-1} nm^{12})	Charge (e)
Cl^{-1}	0.0128097124	6.0466176e-05	-1
Na^+	7.884019264e-05	7.290000e-08	1

S3. Optimization before formal simulation

S3.1. Energy minimization

As shown in Figure S1, the total potential energy at the end of the minimization process was observed to negative, which was expected for a system containing water molecules. From Table S2, the maximum force exerted in all simulated systems was below 200 kJ·mol^{-1}·nm^{-1}, indicating the complete convergence of the energy minimization.[5,6]

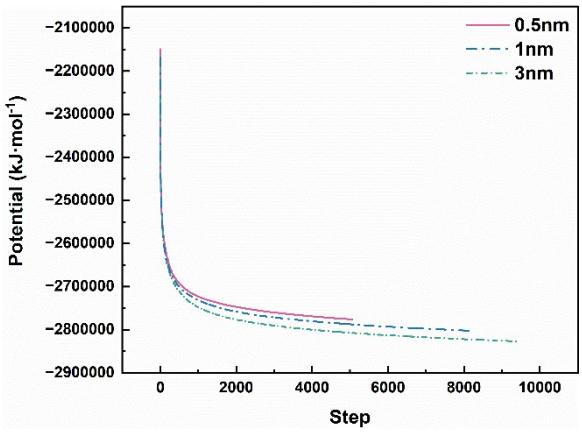

Fig. S1. Potential energy in the process of energy minimization.

Table S2 Data related to energy minimization of the system.

Different transition layer thickness systems	Maximum force (F_{max}) [kJ·(mol·nm)$^{-1}$]	Steps converged to F_{max} < 200	Potential Energy (kJ·mol^{-1})
0.5nm	190.74	9798	-2779700
1nm	150.51	11031	-2802544
3nm	101.17	11406	-2826955

S3.2. Equilibrium

As shown in Figures S2 and S3, the final temperature and pressure of the two systems basically fluctuated slightly around the preset value through the thermostat and barostat. Figure

S4 showed that the total potential energy of the system was stable after equilibrium. So, it was suggested that the balanced structure could be used for formal simulations.[5,6]

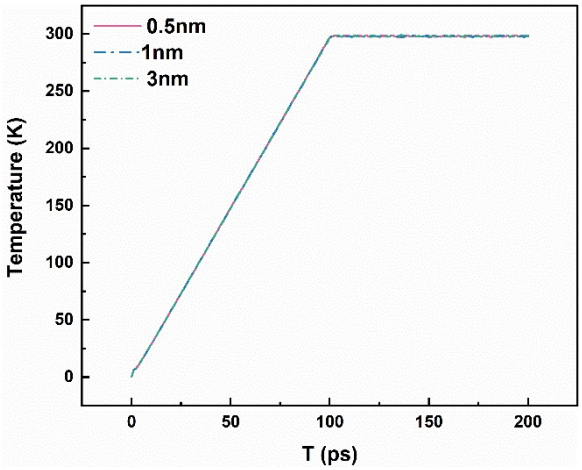

Figure. S2. Temperature during equilibrium.

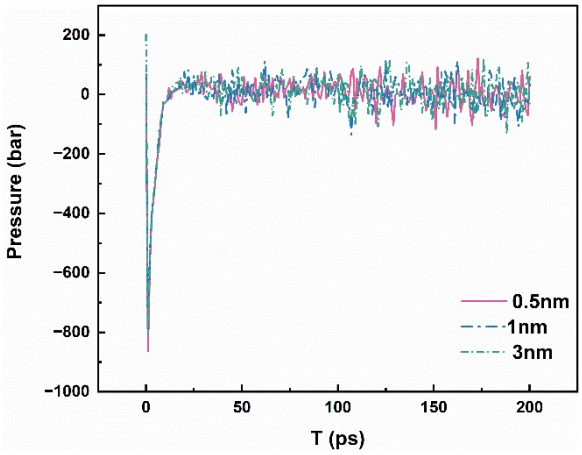

Figure. S3 Pressure during equilibrium.

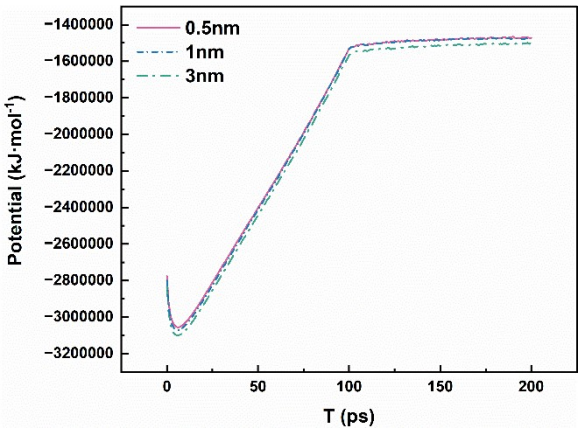

Figure. S4. Potential energy during equilibrium.

S4. Solvent accessible surface area (SASA)

The solvent molecule approaches the van der Waals surface of the central molecule, and the surface through which the center of the solvent molecule passes is referred to as the solvent accessible surface area (SASA), denoted in Figure S5.

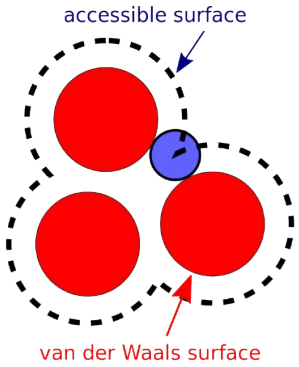

Figure. S5. Schematic diagram of solvent accessible surface area.

The formula for calculating the solvent accessible surface area is as follows.

$$SASA = 4\pi \sum_i r_i^2 \frac{m_{acc}(i)}{m} \tag{S2}$$

where r_i is the sum of the van der Waals and solvent radii for each respective atom, $m_{acc}(i)$ is the number of dots on atom i not occluded by neighboring atoms and the summation is over all atoms in the molecule, and m is the number of points per sphere.

S5. Radius of gyration (Rg)

The radius of gyration is the root-mean-square distance between the atoms in a molecule and their common center of mass. We utilized the "gyrate" command in the GROMACS program to compute the droplet's radius of rotation, also referred to as the contour radius (Rc). The equation for calculating the contour radius is as follows.

$$Rc = \sqrt{\frac{\sum_i m_i \left(r_i - r_c\right)^2}{\sum_j m_j}} \quad \text{(S3)}$$

where m_i, m_j is the mass of the atom, r_i is the coordinate of the atom i, and r_c is the center-of-mass coordinate.

S6. Hydrogen-bond lifetime calculation

The hydrogen-bond lifetime was calculated using the gmx hbond module in GROMACS based on hydrogen-bond autocorrelation analysis. In this work, hydrogen bonds were identified according to the geometric criterion implemented in GROMACS, with a donor–acceptor distance smaller than 0.35 nm and a hydrogen–donor–acceptor angle smaller than 30°. OH and NH groups were treated as hydrogen-bond donors, and oxygen atoms were treated as acceptors.[7,8] The hydrogen-bond lifetime was used to evaluate the dynamic stability of the hydrogen-bond network in different transition-layer systems under the applied electric field.

$$C(\tau) = \left\langle s_i(t) s_i(t+\tau) \right\rangle \quad \text{(S4)}$$

Here, $C(\tau)$ is the hydrogen-bond autocorrelation function, and $s_i(t)$ is the existence function of the ith hydrogen bond. When the hydrogen bond exists at time t, $s_i(t)$ =1; otherwise, $s_i(t)$ =0. This function was used to describe the temporal persistence of hydrogen bonds during the simulation.

$$\tau_{HB} = \int_0^\infty C(\tau) d\tau \quad \text{(S5)}$$

Here, τ_{HB} is the hydrogen-bond lifetime, which was obtained by integrating the autocorrelation function over time. The calculated value reflects the average survival time of hydrogen bonds and was used to compare the stability of hydrogen-bond networks in different systems.

S7. Interaction energy calculation

The intermolecular interaction energy between different components was obtained from the non-bonded interaction terms recorded in the GROMACS energy file. During the simulation setup, different molecular species were defined as separate energy groups, so that the short-range electrostatic interaction energy and short-range van der Waals interaction energy between group pairs could be extracted from the .edr file through the energygrps option.[11,12] The interaction energy was then used to evaluate the relative interaction strength between different transition-layer components.

$$E_{int}(A,B) = E_{Coul-SR}(A,B) + E_{LJ-SR}(A,B) \tag{S6}$$

Here, $E_{int}(A,B)$ is the total interaction energy between component A and component B, $E_{Coul-SR}(A,B)$ is the short-range electrostatic interaction energy between the two components, and $E_{LJ-SR}(A,B)$ is the short-range van der Waals interaction energy between them.

$$\overline{E}_{int}(A,B) = \frac{1}{N}\sum_{k=1}^{N} E_{\text{int}}^{(k)}(A,B) \tag{S7}$$

Here, $\overline{E}_{int}(A,B)$ is the average interaction energy between component A and component B over the selected analysis interval, N is the number of sampled frames, and $E_{\text{int}}^{(k)}(A,B)$ is the instantaneous interaction energy at the kth frame. The average value was used to compare the relative variation in interaction strength among different components in the transition layer.

References

(1) C. Caleman and D. van der Spoel, Picosecond melting of ice by an infrared laser pulse: A simulation study, *Angew. Chem., Int. Ed.*, 2008, **47**, 1417-1420.

(2) M. Stroet, B. Caron, K. M. Visscher, D. P. Geerke, A. K. Malde and A. E. Mark, Automated Topology Builder Version 3.0: Prediction of Solvation Free Enthalpies in Water and

Hexane, *J. Chem. Theory Comput.*, 2018, **14**, 5834-5845.

(3) N. Schmid, A. P. Eichenberger, A. Choutko, S. Riniker, M. Winger, A. E. Mark and W. F. van Gunsteren, Definition and testing of the GROMOS force-field versions 54A7 and 54B7, *Eur. J. Mech. B/Fluid*, 2011, **40**, 843-856.

(4) Li N, Pang Y, Sun Z, et al. Effects of surfactants on droplet deformation and breakup in water-in-oil emulsions under DC electric field: A molecular dynamics study[J]. Fuel, 2024, 358: 130328.

(5) P. S. Lee, R. T. Bradshaw, F. Marinelli, K. Kihn, A. Smith, P. L. Wintrode, D. J. Deredge, J. D. Faraldo-Gómez and L. R. Forrest, Interpreting Hydrogen-Deuterium Exchange Experiments with Molecular Simulations: Tutorials and Applications of the HDXer Ensemble Reweighting Software [Article v1.0], *Living J. Comp. Mol. Sci.*, 2018, DOI: 10.33011/livecoms.3.1.1521.

(6) M. J. Abraham, T. Murtola, R. Schulz, S. Páll, J. C. Smith, B. Hess and E. Lindahl, GROMACS: High performance molecular simulations through multi-level parallelism from S10laptops to supercomputers, *SoftwareX*, 2015, **1**, 19-25.

(7) A. Luzar and D. Chandler, Hydrogen-bond kinetics in liquid water, *Nature*, 1996, **379**, 55-57.

(8) A. Luzar, Resolving the hydrogen bond dynamics conundrum, *J. Chem. Phys.*, 2000, **113**, 10663-10675.